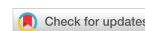


Research Article

Open Access



Data-based interpretation of emerging contaminants occurrence in rivers using a simple advection-reaction model

Antonio Ginebreda¹, Damià Barceló^{1,2}

¹IDAEA, CSIC, Jordi Girona 18-26, Barcelona 08034, Spain.

²ICRA-CERCA, Catalan Institute for Water Research, Scientific and Technologic Park of the UdG, Girona 17003, Spain.

Correspondence to: Prof. Antonio Ginebreda, IDAEA, CSIC, Jordi Girona 18-26, Barcelona 08034, Spain. E-mail: agmqam@cid.csic.es

How to cite this article: Ginebreda A, Barceló D. Data-based interpretation of emerging contaminants occurrence in rivers using a simple advection-reaction model. *Water Emerg Contam Nanoplastics* 2022;1:12. <https://dx.doi.org/10.20517/wecn.2022.07>

Received: 27 May 2022 **First Decision:** 20 Jun 2022 **Revised:** 29 Jun 2022 **Accepted:** 11 Jul 2022 **Published:** 14 Jul 2022

Academic Editor: Teresa A.P. Rocha-Santos **Copy Editor:** Haixia Wang **Production Editor:** Haixia Wang

Abstract

Our knowledge of the river's qualitative status generally relies on discrete spatial and temporal observations organized under what is commonly known as a "monitoring network". Network performance is constrained by its spatial - temporal resolution, which is severely limited by the costs associated with the whole sampling and analytical process. Alternatively, modeling allows predicting the spatial - temporal variable profile at any resolution at affordable computing costs. However, it involves high uncertainty in the parameterization and requires experimental validation as well. Here, we aimed at reconciling monitoring and modeling, deriving simple steady-state advection-reaction (reactive-transport) models from monitoring data. They are based on graph-theoretical concepts, notably the use of the Laplacian matrix, which captures the river network topology, the interaction between adjacent sites, and the advection process between them. The local reactive process is described by a first-order decay reaction. The application of these models provided relevant information about the variables monitored, such as the local dynamics, the distance of the site's influence, the degree of synchronization, or the external input/output to the system, which is useful for both scientific and management purposes.

The model was tested in the Llobregat River (NE Spain) basin, with 70 emerging contaminants of different classes (pharmaceuticals, pesticides, perfluorinated substances, endocrine disruptors, and drugs of abuse). The monitoring network included 14 sites (7 in the mainstream, 4 in the Cardener, and 3 in the Anoia tributaries) and was



© The Author(s) 2022. **Open Access** This article is licensed under a Creative Commons Attribution 4.0 International License (<https://creativecommons.org/licenses/by/4.0/>), which permits unrestricted use, sharing, adaptation, distribution and reproduction in any medium or format, for any purpose, even commercially, as long as you give appropriate credit to the original author(s) and the source, provide a link to the Creative Commons license, and indicate if changes were made.



monitored in 2 campaigns. These models can help water managers to optimize the design of river monitoring networks, a key aspect of environmental regulations.

Keywords: Monitoring network, emerging contaminants, advection-reaction, reactive transport, graph theory, Laplacian matrix

INTRODUCTION

Rivers are net receivers of both point and diffuse pollution, such as nutrients, metals, emerging pollutants, *etc.*^[1], which are considered one of the main causes of freshwater biodiversity impairment^[2,3]. Many chemical pollutants are not environmentally persistent; rather, they change due to multiple biotic (biodegradation) and abiotic processes (sorption, photolysis, hydrolysis, *etc.*), giving rise to additional transformation products. Rivers extend more or less continuously through space and time under the influence of their catchment area. However, only a few variables can be measured with the highest resolution in time (i.e., online sensors) or space (i.e., remote sensing), and none in both dimensions^[4]. Therefore, our knowledge of the river's qualitative status relies on discrete spatial and temporal observations of a set of physical, chemical, or biological parameters, organized under what is commonly known as a “monitoring network” [Figure 1]. Monitoring networks are typically constituted by several sites deployed throughout the river basin area, which are sampled at a certain time-frequency. This is a current practice used for either research or management purposes and has given rise to large databases. Indeed, monitoring networks are a key aspect of the implementation of environmental regulations such as the EU Water Framework Directive (Directive 2000/60/EC). The accuracy of the “picture” obtained depends on both the spatial and temporal “resolution” of the network used. However, it is constrained by the economic cost of the whole sampling and analytical process, often expensive, as is the case of emerging contaminants. To cope with the inherent limitations of discrete monitoring networks, dynamic modeling of chemical fate and transport processes was raised as a complementary alternative^[5]. While both approaches - monitoring and modeling - have their respective pros and cons, there is a growing interest in the latter due to the increasing development and affordability of computation and information techniques compared to costly monitoring campaigns^[5,6]. Modeling approaches have been mostly focused on the prediction of environmental concentrations of pollutants. Existing models include GREAT-ER^[7,8], PhATE^[9], LF2000-WQX^[10,11], and MERLIN-EXPO^[12], among others^[13-16]. However, advanced modeling is not exempt from limitations. They are “data-hungry” and require combining a hydrological model with that of the physical - chemical processes taking place in the river, whose parameterization is often subjected to high uncertainty^[17] that depends on local conditions^[18-20]. Moreover, they ultimately need to be validated through experimental measurements. Altogether, monitoring and modeling must be regarded as complementary tools that should be advantageously used together^[5,21].

Although the use of spatial (topological) relationships in the study of rivers is not new^[21-27], here, we explore new possibilities for exploitation of experimental data available from river monitoring networks, and their interpretation in the light of simple reactive-transport (or advection-reaction) that can be readily derived therefrom. To do so, we make use of some graph-theoretical concepts recently used in the development of models (oscillation models) applied in other domains such as social networks (Internet networks, *etc.*)^[28,29].

The proposed advection-reaction model approach was tested using an available dataset that includes concentrations of *ca.* 70 emerging contaminants belonging to several chemical families and sampled alongside the Llobregat River (NE Spain) during 2010-2011 as part of the project SCARCE^[30].

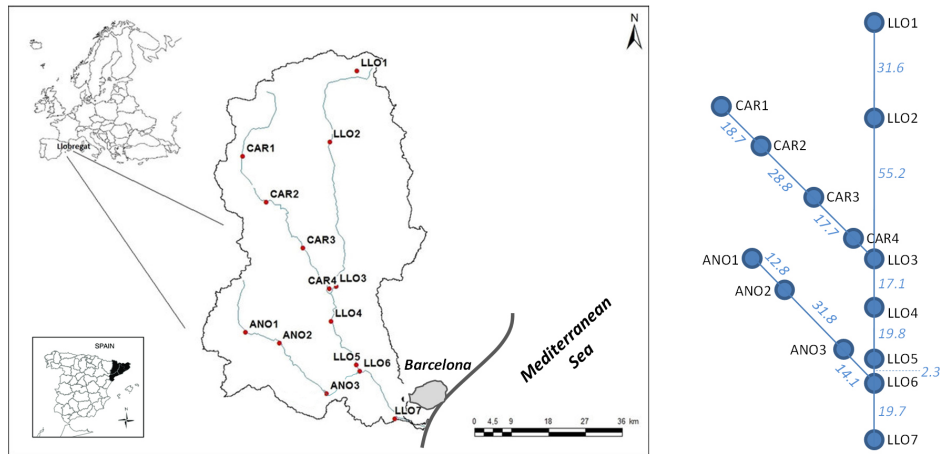


Figure 1. (A) Map of the Llobregat River basin showing the sampling sites. (B) Network graph representation of the area studied. The distances (km) between adjacent sites are indicated in blue.

MATERIALS AND METHODS

Study area

The Llobregat River (NE Spain)^[31] is 156 km long and covers a catchment area of about 4957 km² [Figure 1]. From the hydrologic point of view, the Llobregat is a typical Mediterranean river, its flow being characterized by high variability, which is closely controlled by seasonal rainfall. The mean annual precipitation is 3330 Hm³, and it has an annual average discharge of 693 Hm³. Its watershed is heavily populated with more than three million inhabitants, mostly in the lowest part located in the surroundings of the city of Barcelona. Together with its two main tributaries, River Cardener and River Anoia, the Llobregat is subjected to heavy anthropogenic pressure, receiving extensive urban and industrial wastewater discharges (137 Hm³/year; 92% coming from the wastewater treatment plants), which constitutes a significant part of its natural flow. Overall, 48% of these point sources are located in the studied area. Furthermore, in the middle part of the basin, it receives brine leachates from natural salt formations and mining operations, which have caused an increase in water salinity downstream. The Llobregat is thus an illustrative example of overexploited river.

Advection-reaction model based on network theoretical concepts applicable to a river network of discrete monitoring measurements

Network theory concepts

The river studied can be described as a set of spatially distributed connected sites (nodes) in which we carry out measurements of a variable x (e.g., the concentration of a contaminant) at a certain time, which constitute the monitoring network [Figure 1]. Its structure is conveniently described^[28,29] by a graph $G(E, V)$, where $V = \{1, \dots, n\}$ denotes the set of n nodes representing the monitoring sites and E is the set of edges between nodes. The network structure of nodes and links is captured by the adjacency matrix A . It is an $n \times n$ square defined as:

$$A_{ij} := \begin{cases} 1 & \text{if } (i, j) \in E \\ 0 & \text{otherwise} \end{cases}$$

We define the degree d_i of node i ($i = 1, \dots, n$) as:

$$d_i = \sum_{j \in \theta_i} A_{ij}$$

where v_i denotes the set of nodes adjacent (connected) to node i . The weighted degree matrix \mathbf{D} can be thus defined as:

$$\mathbf{D} := \text{diag}(d_1, \dots, d_n)$$

The so-called graph Laplacian matrix is defined as:

$$\mathbf{L} = \mathbf{D} - \mathbf{A}$$

The elements of \mathbf{L} are given by:

$$L_{ij} \begin{cases} d_i & \text{if } i = j \\ -1 & \text{if } i \neq j \text{ and there is an edge } (i, j) \in E \\ 0 & \text{otherwise} \end{cases}$$

The Laplacian matrix \mathbf{L} is real, symmetric, and semi-definite positive, with all the eigenvalues nonnegative, being always the first eigenvalue $\lambda_1 = 0$ the smallest one and its associated eigenvector $\mathbf{v}_1 = (1, 1, \dots, 1)^T$. This vector corresponds to the fully synchronized state, in which the variable studied x has the same value in all the nodes (i.e., $x_1 = x_2 = \dots = x_{n-1} = x_n$).

The network advection-reaction model

The model provides a simple and general description capturing the network dynamics. Briefly, let the state of node i be x_i so that $\mathbf{x} := (x_1, \dots, x_n)^T$ is the n -dimensional state vector of measurements of variable x for all the nodes. It is assumed that the time evolution of x_i can be described by the following simple kinetic equation:

$$\frac{dx_i}{dt} = -k \cdot x_i + \bar{v} \cdot \sum_{j=1}^n A_{ij}(x_i - x_j) + \delta_i = -k \cdot x_i + \bar{v} \cdot \sum_{j=1}^n L_{ij}x_j + \delta_i \quad (1)$$

where the first term on the right side of the equation reflects a first-order decay process with a rate constant k and the second term is an advection process between the sites connected, characterized by a mean advection velocity \bar{v} (see comment below). The terms δ_i are local inputs or sinks at each site i . We assume that, for a given compound, the rate constants k and the advection velocities v are equal throughout all the space (i.e., alongside the n measurement sites), although they may change at each sampling time. These are common assumptions in many models.

It can be written in the following compact vector form:

$$\dot{\mathbf{x}} = -k \cdot \mathbf{x} + \bar{v} \cdot \mathbf{Lx} + \boldsymbol{\delta} \quad (2)$$

Assuming that the measurements correspond to a stationary state ($\dot{\mathbf{x}} = 0$), rearranging the above equation, and dividing both sides by k , it becomes:

$$\mathbf{x} = \bar{v}/k \cdot \mathbf{L}\mathbf{x} + \delta/k \quad (3)$$

Numerically, the parameter \bar{v}/k could be assimilated to the slope of the regression line of $\mathbf{L}\mathbf{x}$ over \mathbf{x} with the intercept set equal to 0. Its calculation can be readily done by ordinary least squares (OLS), and the vector $\varepsilon = \delta/k$ of errors ($\varepsilon = \mathbf{x} - \bar{v}/k \cdot \mathbf{L}\mathbf{x}$) captures the local input/output (under the OLS assumptions).

It can be shown that the inverse of the OLS calculated slope ($\rho = k/\bar{v}$) is equal to:

$$\rho = \frac{\mathbf{x}^T \mathbf{L}\mathbf{x}}{\mathbf{x}^T \mathbf{x}} \quad (4)$$

Noting that the right-hand expression in the above equation is the Rayleigh quotient of the Laplacian matrix \mathbf{L} (https://en.wikipedia.org/wiki/Rayleigh_quotient), for any vector \mathbf{x} , ρ is bounded between its minimum and maximum eigenvalues, so that:

$$0 \leq \rho \leq \lambda_{max}$$

Furthermore, expanding \mathbf{x} in terms of the normalized eigenvectors \mathbf{u} of \mathbf{L} , and considering that $c_i = \mathbf{u}_i^T \mathbf{x}$ (graph Fourier transform of \mathbf{x}), we have the following expression that quantifies the contribution of the different eigenstates λ_i to ρ :

$$\rho = \sum_i c_i^2 \lambda_i \quad (5)$$

with $\sum_i c_i^2 = 1$ Equation (6). This allows defining an entropy S as:

$$S = -\sum_i c_i^2 \ln c_i^2 \quad (6)$$

Entropy S provides an insight into how the ρ is allocated among the different eigenstates. In turn, the terms c_i^2 capture [Equation (5)] the respective contribution of each eigenstate i . For our purposes, the first one is particularly relevant, namely c_1^2 , the eigenstate associated with the first eigenvalue $\lambda_1 = 0$, which quantifies the weight of the synchronized state (note, however, that the contribution of the synchronized state to ρ is zero since $\lambda_1 = 0$).

Definition of the “weighted” Laplacian for practical use

Without loss of generality, the foregoing definitions of the adjacency and Laplacian matrices can be extended to “weighted” analogs, i.e., $A_{ij} = w_{ij}$, that better capture real problems. Here, the weight associated with the edge (i, j) w_{ij} of the aquifer weighted adjacency matrix elements was set equal to the inverse of the distance r_{ij} between connected sites i and j : $w_{ij} = 1/r_{ij}$ (dimension L^{-1}). Defined in this way, it is worth noting that the terms $(x_i - x_j)/r_{ij}$ in Equation (1) can be regarded as the discrete counterparts of a gradient $\partial x/\partial r$. Hence, the term \bar{v}/k has the dimension L and can be interpreted as a *characteristic length* (referred to hereafter as ℓ). In addition, \bar{v}/k may be interpreted as a measure of the relative relevance of the two

processes involved, i.e., advection (between neighbor nodes) and decay (local at each node). Likely, the vector $\varepsilon = \delta/k$ has the dimension of concentration [Equation (3)] and provides information on the local inputs/output of the x variable.

Calculations

All the calculations were performed using Excel (Microsoft®) and the R environment (version 4.1.0). Measurements below the limit of detection (< LOD) and the limit of quantification (< LOQ) were set equal to 0 for calculation purposes.

Monitoring of emerging contaminants

The sampling of water for chemical characterization was performed at the end of the summer period in campaigns carried out in autumn for two consecutive years, namely 2010 (C1) and 2011 (C2). Sampling sites (14) were distributed in the Llobregat mainstream (seven sites), and the Cardener and Anoia tributaries (four and three sites, respectively) [Figure 1]. At each site, grab water samples were taken for chemical analyses of the organic micropollutants. In total, 199 organic micropollutants were measured using previously published analytical methods based on gas chromatography-tandem mass spectrometry or liquid chromatography - tandem mass spectrometry for pesticides^[32], pharmaceuticals^[33], endocrine-disrupting chemicals (EDCs) and related compounds (hormones, plasticizers, alkylphenols, parabens, phosphate flame retardants, anticorrosion agents, and bactericides)^[34], perfluorinated compounds^[35,36], and drugs of abuse^[37].

To avoid an excessive number of “0 values” (i.e., not detected or not quantified), the above-described methods were applied to compounds having detection frequencies equal to or greater than 20% in each of the two sampling campaigns performed, which resulted in a final selection of 71 compounds out of the 199 monitored [Supplementary Table 1].

RESULTS AND DISCUSSION

Monitoring information (limits of detection, detection frequency, and mean and maximum concentrations) corresponding to the selected compounds and the two campaigns are collected in Supplementary Table 1. Compounds were grouped per class as follows: drugs of abuse (5), endocrine disruptors (13), perfluorinated compounds (6), pesticides (6), and pharmaceuticals (37). A full description and discussion of monitoring results^[32-37] and their associated ecotoxicological risk^[38,39], as well as their relationship with the receiving ecosystems^[1,40,41], was previously published.

Advection-reaction network models

The application of the above-described advection-reaction model (Section “Study area”) to each of the 71 compounds selected provided as main quantitative outputs the following information: (a) characteristic distances (ℓ) [Equation (3)]; (b) entropy [Equation (6)]; (c) local input/outputs [Equation (3)]; and (d) the contribution of the different eigenstates [Equation (5)]. Although these quantitative indicators are not fully independent and exhibit some quantitative relationships (see below), they provide somewhat complementary information useful for different interpretation purposes. Whereas the characteristic length ($\ell = \bar{v}/k$) gives an idea of the distance through which the advection process is effective compared to the decay process, its inverse [$\rho = x^T L x / x^T x$, Equation (4)] is often referred to in graph theory as the “network energy”. Finally, its spectral decomposition in terms of the eigenvectors and eigenvalues of L allows us to describe it as a superposition (sum) of the different eigenstates (modes) contained in L [Equation (5)]. Among the latter, the contribution of the fully synchronized state, in which all sites have the same concentration for the variable under study, is particularly relevant, since it corresponds to the equilibrium state in which the concentration of the measured variable is the same in all sites. Finally, the relative

contribution of each eigenstate to ρ (“network energy”) is conveniently captured by an entropy [Equation (6)] (the parallelism of the foregoing definitions with the corresponding thermodynamic concepts is rather evident). The statistical distributions of characteristic lengths (ℓ), entropies, and synchronized state contribution are shown in [Figure 2A-C](#), respectively, for the different families of compounds and sampling campaigns. Characteristic lengths of the whole compound set were between 123 and 2.3 km, with a median of 16.4 km. This value is of the same order as the distance between adjacent monitoring sites (mean, 20.6 km; max, 55.2; min, 2.3 km; median, 18.2 km), meaning that the monitoring network fits the requirements reasonably well. In that sense, the characteristic lengths provide a relevant insight for the optimization of monitoring networks, whose separation between sites should ideally take into consideration the range of lengths of the set of compounds monitored (notably those with the shortest ones). In general, ℓ values in campaign C1 were larger than those in C2 for all the compound classes [[Figure 2A](#)], with more pronounced values and differences between campaigns corresponding to pesticides and perfluorinated compounds. Such small but perceptible differences could possibly be explained through corresponding variations in hydrology. Thus, for instance, whereas the autumn of 2010 was characterized by intense precipitation which resulted in a high flow, the autumn of 2011 was dry and the river flows were comparatively lower. High flows give rise to larger linear velocities and, hence, longer characteristic lengths, which tend to increase the contribution of the advection process, thus improving the river connectivity. This pattern (and its hydrological explanation) is also reflected in the increasing contribution of the synchronized state [[Figure 2C](#)]. It is worth noting that, in a hypothetical fully synchronized (i.e., 100%) situation, $\rho = 0$ [Equation (3)], and its inverse, the characteristic length ℓ , would thus be infinite. In that sense, the contribution of the synchronized state is typically higher in C1 than in C2, with maximum differences occurring in the case of pesticides.

Entropy values for the different compound classes are given in [Figure 2B](#). They show the lowest values for pesticides and appear systematically lower in C1 than in C2. Entropy captures the system “complexity”, providing a quantitative measure of how the different eigenstates of the Laplacian matrix contribute to the description of the system. Entropy takes its maximum value when all the states are equally allocated. High entropy values thus reflect a heterogenous hydrological environment and would be indicative of a “fragmented” situation, as happens under water scarcity, typical of Mediterranean rivers^[42].

As mentioned above, the three properties studied exhibit related trends, which are depicted in [Figure 3A](#) and [B](#). Overall, the characteristic length has a negative correlation with entropy (Pearson correlation = -0.748, [Figure 3A](#)), while synchronization shows a positive one (Pearson correlation = 0.561, [Figure 3B](#)).

Further analysis of the processes involved can be achieved considering the respective contributions of the different eigenstates of the Laplacian matrix L to Equations (5) and (6). Specifically, the contribution of the synchronized state (i.e., equal values of measured pollutant x in all nodes) *vs.* higher states is relevant, considering that a fully synchronized state would have $\rho = 0$ [Equation (5)], and thus an infinite characteristic length. In that sense, as one may expect, synchronization was aligned with a characteristic length [[Figure 2A](#)]. Focusing on the individual compounds, the highest values and differences between campaigns of characteristic lengths [[Figure 4A](#)] were found in some pesticides (chlorpyrifos, imazalil, and diazinon), perfluorinated compounds (PFOA and PFPeA), and pharmaceuticals (non-steroidal antiinflammatories naproxen, ibuprofen, ketoprofen, and meloxicam), with notably higher values in the 2010 campaign (C1).

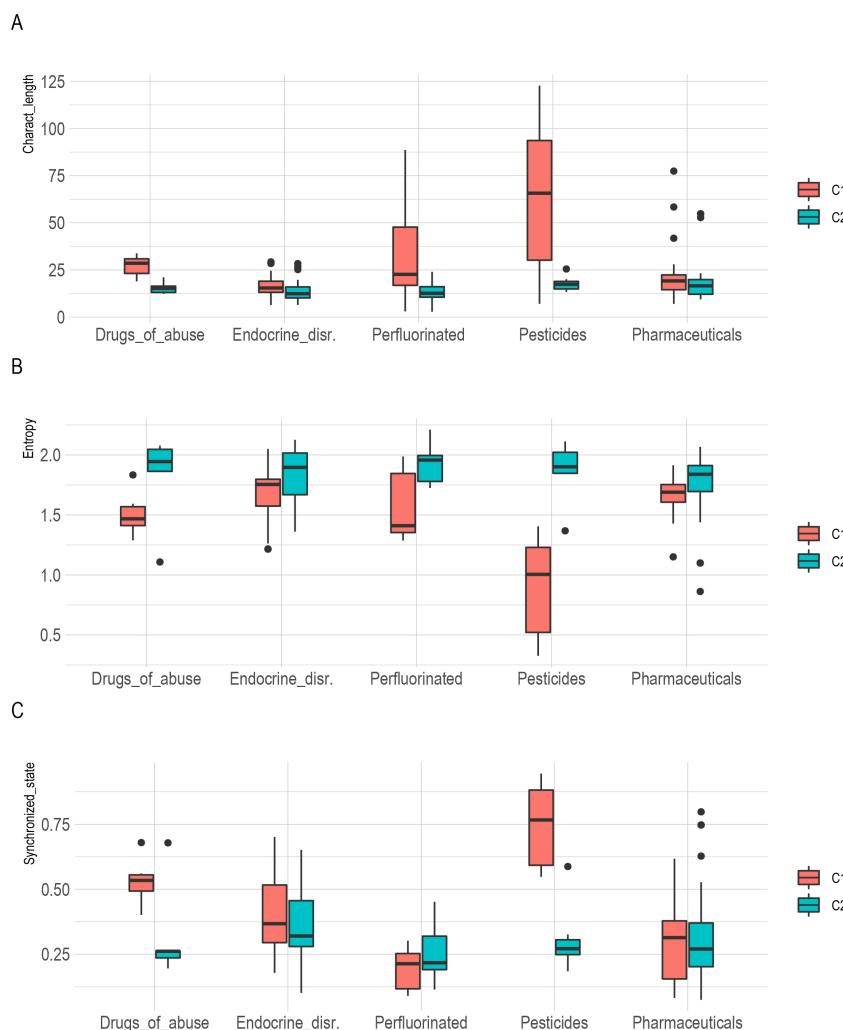


Figure 2. Boxplots showing the distribution of the values per sampling campaign (C1, 2010; C2, 2011) for the different compound classes: (A) characteristic length (km); (B) entropy; and (C) synchronized state contribution. The upper and lower bounds correspond to maximum and minimum values; boxes are limited by the 75th and 25th quartiles; and dots correspond to outliers.

Contrastingly, entropy values were generally higher in 2011 (C2) than in 2010 (C1) [Figure 4B], with the largest differences corresponding to the group of pesticides (isoproturon, imazalil, diazinon, and chlorpyrifos), while the synchronization showed a mixed situation [Figure 4C].

Relevant information regarding the input/output pollution load throughout the basin can be obtained from the vector $\varepsilon = \delta/k$ of Equation (3), whose components' signs provide insight into each sampling site's behavior, indicating if it is a net receiver (positive) or a sink (negative) of pollution. Figure 5 shows some examples, including the total pollution per site along with the two campaigns C1 and C2 (i.e., the variable x was the aggregated sum of all pollutants measured at a site) [Figure 5D], as well as some individual compounds representative of the different sources of pollution, namely the anticorrosion agent 1H-benzotriazole (industrial), the insecticide chlorpyrifos (agriculture), and the pharmaceutical diclofenac (urban) (Figure 5A-C, respectively). Concerning the absolute input/output quantities, the observed order was: sum of all pollutants > 1H-benzotriazole > diclofenac > chlorpyrifos. Each one exceeded the next by circa one order of magnitude. Both campaigns showed similar input/output profiles for chlorpyrifos and

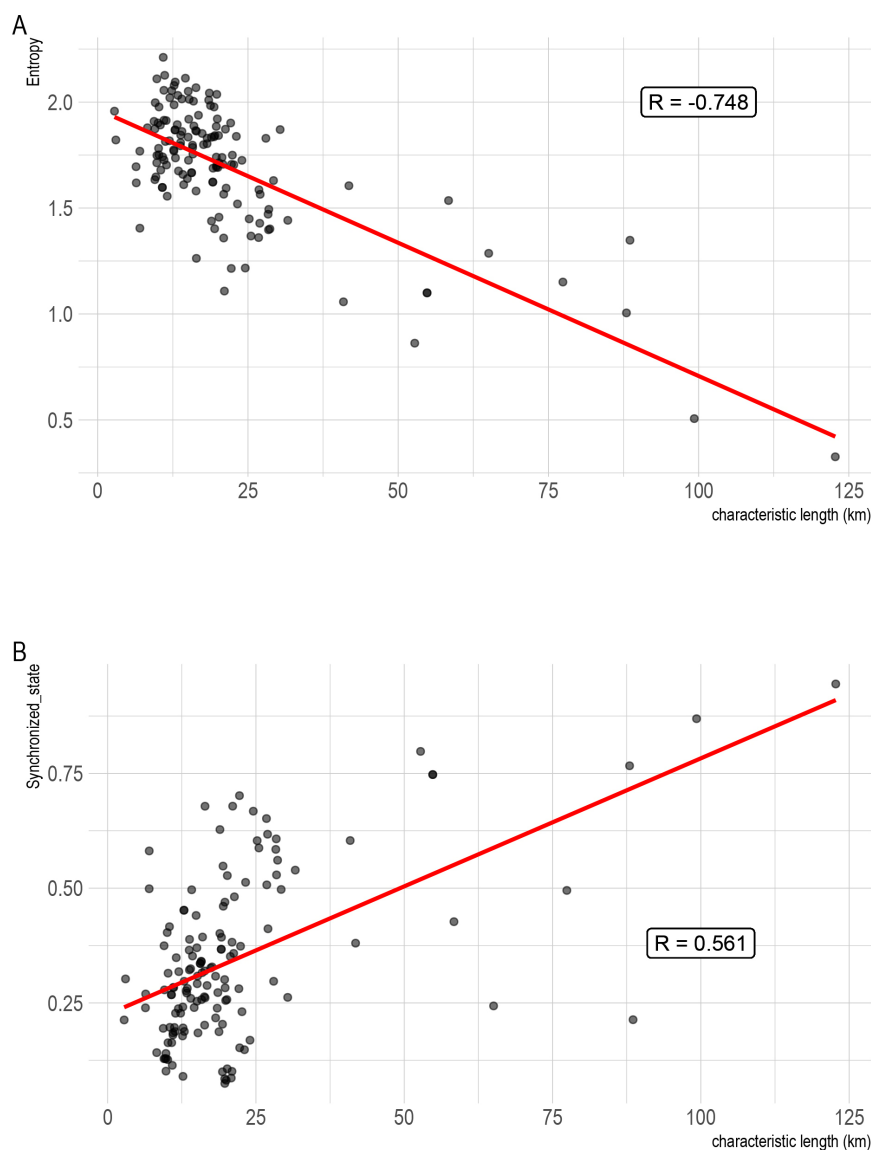


Figure 3. Scatter plots showing the relationships between characteristic length and entropy as well as synchronized state of all compounds studied in the two campaigns ($n = 142$): (A) characteristic length (km) vs. entropy; and (B) characteristic length (km) vs. synchronized state contribution.

the sum of all pollutants, while the industrial and urban representatives showed slightly higher input values in C2 than in C1, which is consistent with the hydrology (i.e., lower flow dilution in the former campaign). Input/output patterns per site were roughly similar for the sum of all pollutants, 1H-benzotriazole, and diclofenac, which is consistent with their respective contribution to the total pollutant load. They highlighted some sites such as ANO3 and LLO3 where pollution depletion exceeded the pollution received (negative sign), while others such as ANO1, CAR4, or LLO6 (positive sign) exhibited the opposite behavior, thus indicating that the reception of external sources of pollution exceeded their elimination capacity. The latter two are well-known polluted sites by both industry and urban population sources, located close to the Manresa and Barcelona metropolitan areas, respectively. Some other sites, mainly located in the relatively

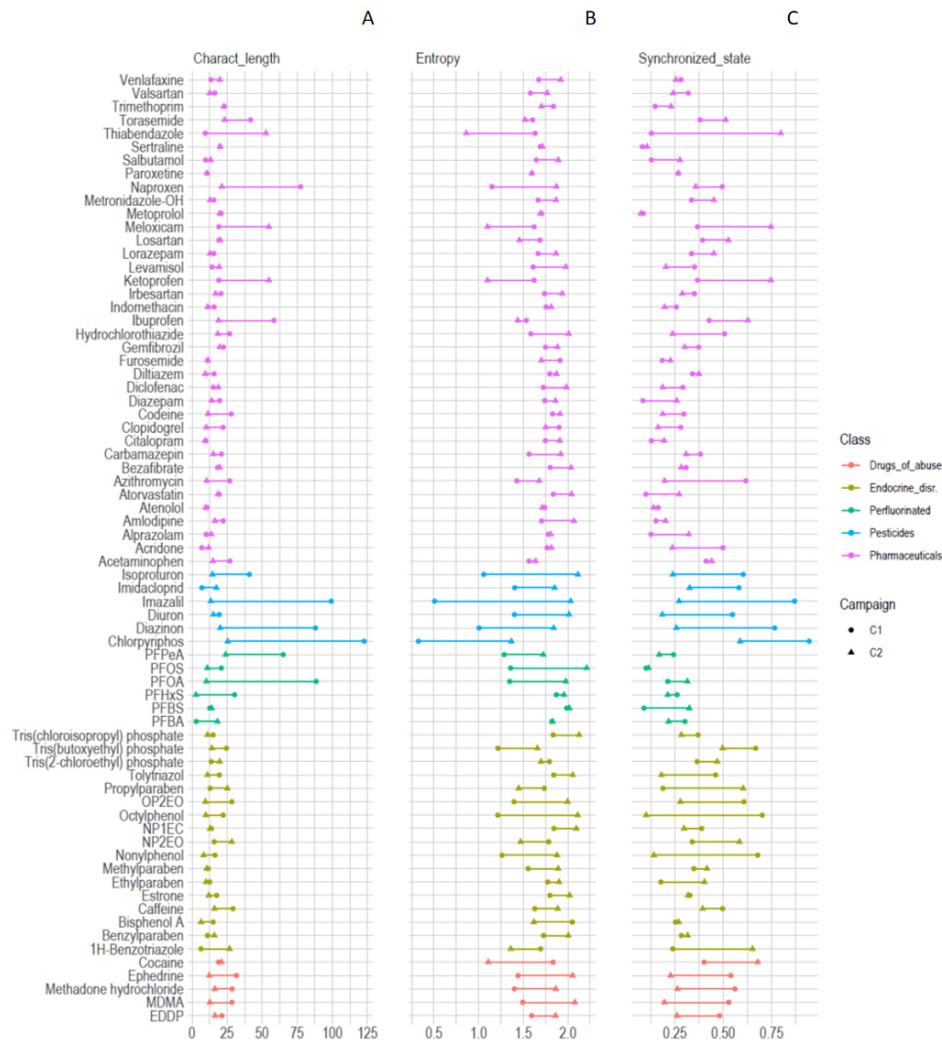


Figure 4. Value distribution per compound along the two sampling campaigns monitored (C1, 2010; C2, 2011): (A) characteristic length (km); (B) entropy; and (C) contribution of the synchronized state (%).

clean upper course of the Cardener tributary (CAR1, CAR2, and CAR3), have a “neutral” behavior, characterized by null values. Contrastingly, the insecticide chlorpyrifos exhibited a somewhat different pattern, spread along the mid and lower river basin, with the largest inputs observed in ANO2, CAR3, LLO3, and LLO6.

CONCLUSIONS

River basin quality status assessment is largely determined through discrete measurements of different variables carried out at certain sites located alongside the catchment and specified time frequencies, under what is usually known as a “monitoring network”. These are currently used for both research and water management purposes and have given rise to large datasets. Network performance is constrained by its spatial-temporal resolution, which, in turn, is severely limited by the, often expensive, costs associated with the whole sampling and analytical process, as in the case of emerging contaminants. Alternatively, modeling allows predicting the spatial-temporal variable profile at any resolution at an affordable computing cost. However, it involves high uncertainty in the parameterization and requires, in the end, experimental

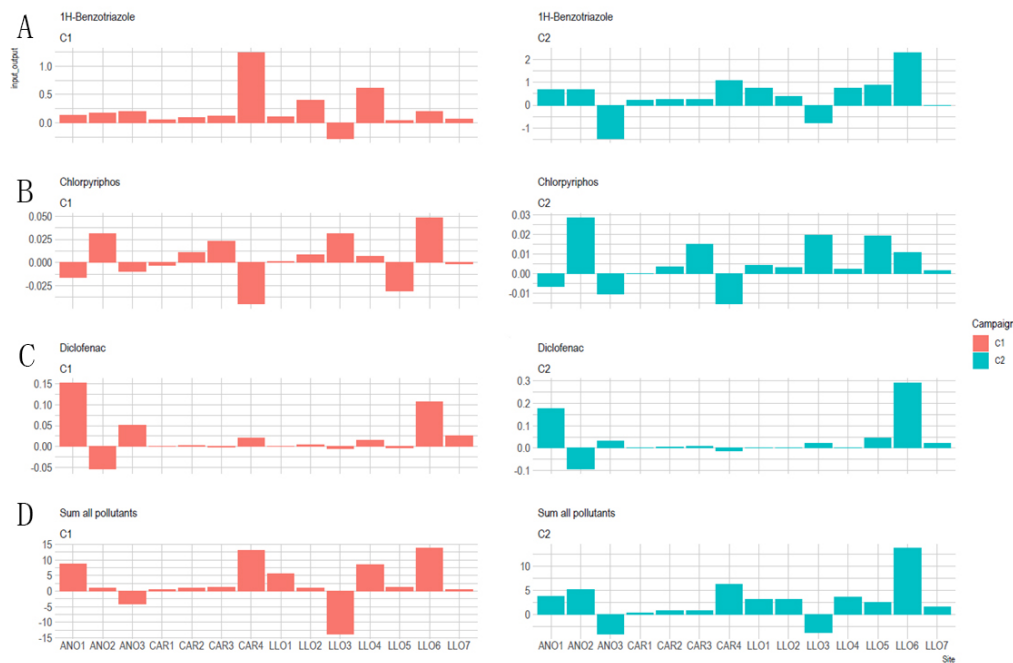


Figure 5. Net input/output per site along the two sampling campaigns monitored (C1, 2010; C2, 2011) at each sampling site of: (A) 1H-benzotriazole (anticorrosion agent, industrial use); (B) chlorpyrifos (insecticide, agriculture use); (C) diclofenac (pharmaceutical, urban use); and (D) total pollution load (expressed as the sum of all pollutants analyzed).

validation.

In the present short contribution, we aimed at reconciling both approaches - monitoring and modeling - through the interpretation of the experimental data under the framework of a simple advection-reaction (i.e., reactive-transport) model based on graph-theoretical concepts, notably the use of the Laplacian matrix, which adequately captures the river network topology and the interaction between adjacent sites. Whereas the Laplacian matrix has been previously used in spatial geographic analysis (e.g., the so-called “Geary coefficient”^[43], a widely used spatial correlation index, can be expressed in terms of the Laplacian matrix^[44]), here we used it for the first time in two novel aspects: (a) to capture the advection process taking place between adjacent sites in the context of an advection-reaction model; and (b) the definition of an entropy that quantifies the contribution of the different eigenstates (modes) of the Laplacian to the measured variable.

Despite their obvious limitations, the approach presented here is straightforward and can provide useful information regarding the dynamics of the variables monitored, such as the local dynamics, the influence of the neighbor sites, the degree of synchronization, or the external input/output to the system. Even though the methods and results presented in this study were specifically concerned with emerging contaminants, they can be easily extended to any other site-measured variables as well, such as nutrients, inorganic constituents, heavy metals, or even biological parameters such chlorophyll, dissolved enzymes (alkaline phosphatase), *etc.*

Finally, since monitoring for water quality assessment is a key aspect in the implementation of environmental legislation, such as the Water Framework Directive (Directive 2000/60/EC), the presented modeling approach can provide valuable insights for water managers engaged in the proper and consistent

design of river monitoring networks, whether surveillance, operational, or investigative, with potential practical consequences on the optimization of economic costs.

DECLARATIONS

Acknowledgment

This work has been supported by the Spanish Ministry of Science and Innovation (MCIN).

Authors' contributions

Involved in the conception: Ginebreda A, Barceló D

Involved in the design, data treatment and interpretation: Ginebreda A

Writing of manuscript and critical reading: Ginebreda A, Barceló D

Availability of data and materials

Data are available at the Supplementary Material [[Supplementary Table 1](#)].

Financial support and sponsorship

This work has been financed by the Spanish Ministry of Science and Innovation (MCIN), through Project SINERGIA included in the Severo Ochoa Grant CEX2018-000794-S funded by MCIN/AEI/10.13039/501100011033.

Conflicts of interest

All authors declared that there are no conflicts of interest.

Ethical approval and consent to participate

Not applicable.

Consent for publication

Not applicable.

Copyrights

© The Author(s) 2022

REFERENCES

1. Sabater S, Barceló D, De Castro-Català N, et al. Shared effects of organic microcontaminants and environmental stressors on biofilms and invertebrates in impaired rivers. *Environ Pollut* 2016;210:303-14. [DOI PubMed](#)
2. Vörösmarty CJ, McIntyre PB, Gessner MO, et al. Global threats to human water security and river biodiversity. *Nature* 2010;467:555-61. [DOI PubMed](#)
3. Malaj E, von der Ohe PC, Grote M, et al. Organic chemicals jeopardize the health of freshwater ecosystems on the continental scale. *Proc Natl Acad Sci U S A* 2014;111:9549-54. [DOI PubMed PMC](#)
4. O'Grady J, Zhang D, O'Connor N, Regan F. A comprehensive review of catchment water quality monitoring using a tiered framework of integrated sensing technologies. *Sci Total Environ* 2021;765:142766. [DOI PubMed](#)
5. Johnson AC, Ternes T, Williams RJ, Sumpter JP. Assessing the concentrations of polar organic microcontaminants from point sources in the aquatic environment: measure or model? *Environ Sci Technol* 2008;42:5390-9. [DOI PubMed](#)
6. Pistocchi A, Marinov D, Pontes S, Gawlik BM. Continental scale inverse modeling of common organic water contaminants in European rivers. *Environ Pollut* 2012;162:159-67. [DOI PubMed](#)
7. Feijtel T, Boeije G, Matthies M, et al. Development of a geography-referenced regional exposure assessment tool for European rivers - great-er contribution to great-er #1. *Chemosphere* 1997;34:2351-73. [DOI](#)
8. Schowanek D, Webb S. Exposure simulation for pharmaceuticals in European surface waters with GREAT-ER. *Toxicol Lett* 2002;131:39-50. [DOI PubMed](#)
9. Anderson PD, D'Aco VJ, Shanahan P, et al. Screening analysis of human pharmaceutical compounds in U.S. surface waters. *Environ Sci Technol* 2004;38:838-49. [DOI PubMed](#)
10. Keller V, Young AR. Development of the Integrated Water Resources and Water Quality Modelling System, Science Report P2-

- 248/SR. The Environmental Agency, Bristol, UK, 2004.
11. Johnson AC, Keller V, Williams RJ, Young A. A practical demonstration in modelling diclofenac and propranolol river water concentrations using a GIS hydrology model in a rural UK catchment. *Environ Pollut* 2007;146:155-65. DOI PubMed
 12. Ciffroy P, Tediosi A, Capri E (Eds.). Modelling the fate of Chemicals in the Environment and the Human Body. The Handbook of Environmental Chemistry, Vol 57. Springer Int. Publ. Switzerland; 2018. Available from: <https://link.springer.com/book/10.1007/978-3-319-59502-3> [Last accessed on 13 Jul 2022].
 13. Pistocchi A, Sarigiannis DA, Vizcaino P. Spatially explicit multimedia fate models for pollutants in Europe: state of the art and perspectives. *Sci Total Environ* 2010;408:3817-30. DOI PubMed
 14. Osorio V, Marcé R, Pérez S, Ginebreda A, Cortina JL, Barceló D. Occurrence and modeling of pharmaceuticals on a sewage-impacted Mediterranean river and their dynamics under different hydrological conditions. *Sci Total Environ* 2012;440:3-13. DOI PubMed
 15. Lindim C, van Gils J, Cousins IT. A large-scale model for simulating the fate & transport of organic contaminants in river basins. *Chemosphere* 2016;144:803-10. DOI PubMed
 16. Acuña V, Bregoli F, Font C, et al. Management actions to mitigate the occurrence of pharmaceuticals in river networks in a global change context. *Environ Int* 2020;143:105993. DOI PubMed
 17. Banjac Z, Ginebreda A, Kuzmanovic M, et al. Emission factor estimation of ca. 160 emerging organic microcontaminants by inverse modeling in a Mediterranean river basin (Llobregat, NE Spain). *Sci Total Environ* 2015;520:241-52. DOI PubMed
 18. Kunkel U, Radke M. Reactive tracer test to evaluate the fate of pharmaceuticals in rivers. *Environ Sci Technol* 2011;45:6296-302. DOI PubMed
 19. Kunkel U, Radke M. Fate of pharmaceuticals in rivers: deriving a benchmark dataset at favorable attenuation conditions. *Water Res* 2012;46:5551-65. DOI PubMed
 20. Acuña V, von Schiller D, García-Galán MJ, et al. Occurrence and in-stream attenuation of wastewater-derived pharmaceuticals in Iberian rivers. *Sci Total Environ* 2015;503-504:133-41. DOI PubMed
 21. Ginebreda A, Sabater-Liesla L, Rico A, Focks A, Barceló D. Reconciling monitoring and modeling: an appraisal of river monitoring networks based on a spatial autocorrelation approach - emerging pollutants in the Danube River as a case study. *Sci Total Environ* 2018;618:323-35. DOI PubMed
 22. Ort C, Hollender J, Schaerer M, Siegrist H. Model-based evaluation of reduction strategies for micropollutants from wastewater treatment plants in complex river networks. *Environ Sci Technol* 2009;43:3214-20. DOI PubMed
 23. Sabater-Liesla L, Ginebreda A, Barceló D. Shifts of environmental and phytoplankton variables in a regulated river: a spatial-driven analysis. *Sci Total Environ* 2018;642:968-78. DOI PubMed
 24. Mainali J, Chang H, Chun Y. A review of spatial statistical approaches to modeling water quality. *Prog Phys Geogr* 2019;43:801-26. DOI
 25. Rashid A, Amin M, Li Y, et al. Reconciliation of spatiotemporal influences on two-dimensional distribution and fate of emerging contaminants in a subtropical river. *ACS EST Water* 2021;1:2305-17. DOI
 26. Sebestyén V, Czvetkó T, Abonyi J. Network-based topological exploration of the impact of pollution sources on surface water bodies. *Front Environ Sci* 2022;9:723997. DOI
 27. Zhang Y, Rashid A, Guo S, et al. Spatial autocorrelation and temporal variation of contaminants of emerging concern in a typical urbanizing river. *Water Res* 2022;212:118120. DOI PubMed
 28. Aida M, Takano C, Murata M. Oscillation model for describing network dynamics caused by asymmetric node interaction. *IEICE Trans Commun* 2018;E101.B:123-36. DOI
 29. Aida M, Takano C, Ogura M. On the fundamental equation of user dynamics and the structure of online social networks. In: Masuda N, Goh K, Jia T, Yamanoi J, Sayama H, editors. Proceedings of NetSci-X 2020: Sixth International Winter School and Conference on Network Science. Cham: Springer International Publishing; 2020. pp. 155-70. DOI
 30. Navarro-Ortega A, Acuña V, Batalla RJ, et al. Assessing and forecasting the impacts of global change on Mediterranean rivers. The SCARCE Consolider project on Iberian basins. *Environ Sci Pollut Res Int* 2012;19:918-33. DOI PubMed
 31. Eljarrat E, Barceló D. Occurrence and behavior of brominated flame retardants in the Llobregat river basin. In: Sabater S, Ginebreda A, Barceló D, editors. The Llobregat. Berlin: Springer Berlin Heidelberg; 2012. pp. 135-50. DOI
 32. Masiá A, Campo J, Navarro-Ortega A, Barceló D, Picó Y. Pesticide monitoring in the basin of Llobregat River (Catalonia, Spain) and comparison with historical data. *Sci Total Environ* 2015;503-504:58-68. DOI PubMed
 33. Osorio V, Larrañaga A, Aceña J, Pérez S, Barceló D. Concentration and risk of pharmaceuticals in freshwater systems are related to the population density and the livestock units in Iberian Rivers. *Sci Total Environ* 2016;540:267-77. DOI PubMed
 34. Gorga M, Petrovic M, Barceló D. Multi-residue analytical method for the determination of endocrine disruptors and related compounds in river and waste water using dual column liquid chromatography switching system coupled to mass spectrometry. *J Chromatogr A* 2013;1295:57-66. DOI PubMed
 35. Llorca M, Farré M, Picó Y, Müller J, Knepper TP, Barceló D. Analysis of perfluoroalkyl substances in waters from Germany and Spain. *Sci Total Environ* 2012;431:139-50. DOI PubMed
 36. Onghena M, Moliner-Martinez Y, Picó Y, Campins-Falcó P, Barceló D. Analysis of 18 perfluorinated compounds in river waters: comparison of high performance liquid chromatography-tandem mass spectrometry, ultra-high-performance liquid chromatography-tandem mass spectrometry and capillary liquid chromatography-mass spectrometry. *J Chromatogr A* 2012;1244:88-97. DOI PubMed
 37. Mastroianni N, Bleda MJ, López de Alda M, Barceló D. Occurrence of drugs of abuse in surface water from four Spanish river basins:

- spatial and temporal variations and environmental risk assessment. *J Hazard Mater* 2016;316:134-42. [DOI](#) [PubMed](#)
38. Kuzmanović M, Ginebreda A, Petrović M, Barceló D. Risk assessment based prioritization of 200 organic micropollutants in 4 Iberian rivers. *Sci Total Environ* 2015;503-504:289-99. [DOI](#) [PubMed](#)
 39. Kuzmanović M, López-Doval JC, De Castro-Català N, et al. Ecotoxicological risk assessment of chemical pollution in four Iberian river basins and its relationship with the aquatic macroinvertebrate community status. *Sci Total Environ* 2016;540:324-33. [DOI](#) [PubMed](#)
 40. Ponsati L, Corcoll N, Petrović M, et al. Multiple-stressor effects on river biofilms under different hydrological conditions. *Freshw Biol* 2016;61:2102-15. [DOI](#)
 41. Kuzmanovic M, Dolédec S, de Castro-Catala N, et al. Environmental stressors as a driver of the trait composition of benthic macroinvertebrate assemblages in polluted Iberian rivers. *Environ Res* 2017;156:485-93. [DOI](#) [PubMed](#)
 42. Acuña V, Datry T, Marshall J, et al. Conservation. Why should we care about temporary waterways? *Science* 2014;343:1080-1. [DOI](#) [PubMed](#)
 43. Geary RC. The contiguity ratio and statistical mapping. *The Incorporated Statistician* 1954;5:115. [DOI](#)
 44. Yamada H. Geary's c and spectral graph theory. *Mathematics* 2021;9:2465. [DOI](#)